BJRS

BRAZILIAN JOURNAL
OF
RADIATION SCIENCES
09-01A (2021) 01-12

USE OF MONTE CARLO SIMULATIONS FOR OPTIMAL GEOMETRY STUDY IN CALCULATION OF ATTENUATION COEFFICIENT FOR ELEMENT, COMPOUND AND MIXTURE

Barbosa[1,2], C.M.; Raitz[2], C.; Dam[1,2], R.S.F.; Salgado[1,2], W. L.; Salgado[2], C. M, Braz[1],D.

[1] *Universidade Federal do Rio de Janeiro/COPPE/PEN, 21941-614, Rio de Janeiro, RJ, Brazil*

[2] *Instituto de Engenharia Nuclear/CNEN, 21941-906, Rio de Janeiro, RJ, Brazil*

carolmattosb@yahoo.com.br; cbarbosa@nuclear.ufrj.br

ABSTRACT

MCNP is a code extensively used to simulate experiments involving transport of radiation using the Monte Carlo method. This code allows the study of different geometries, materials, and radiation types (e.g. gamma, neutron, and electron), enabling the building of approximate models before the experimental implementation. The objective of this study is to develop an optimal geometry for the calculation of the mass attenuation coefficient for different materials using the MCNP code. Two measurement geometries were tested with different radiation energies, and the best results were obtained using a single lead collimator on the detector and virtual collimation of the source. The considered geometries were isotropic source with lead collimators for source and detector, and a single lead collimator on the detector and virtual collimation of the source. The second case was proposed as a replacement for the computationally time expensive simulation of the first geometry case. The energies 59 keV, 81 keV, 356 keV, and 662 keV were used to model the main gamma emissions from ^{241}Am, ^{133}Ba, and ^{137}Cs radiation sources, respectively. The investigated materials for the target sample were, NaI for the detector, aluminum, water, and artificial seawater (3.5% NaCl). The values of mass attenuation coefficients obtained from the simulations were compared with the NIST XCOM Database ones for validation of the geometries.

ISSN: 2319-0612
Accepted: 2021-03-10

Keywords: **MCNP, Nuclear Technique, gamma ray.**

1. INTRODUCTION

Nuclear techniques are applied in different areas of industry, medicine, and environmental control. It is advantageous to make use of these techniques for they are non-invasive and offer a variety of analysis methods for each problem. With the advance of computational tools, in addition to experimental techniques, we may approach the solution of a problem using simulation tools. For that purpose, the interaction of radiation with materials, with different composition and densities, can be simulated with the Monte Carlo N-Particle (MCNP) code, and the simulation results can be used to calculate the mass attenuation coefficient of those materials.

1.1. MCNP

Monte Carlo N-Particle is a code developed based upon the statistical Monte Carlo method, the MCNP simulates the transport of radiation and particles, neutrons, photons, and electrons, and the processes of interaction of radiation with matter. The applications are in several areas that use nuclear techniques, such as radiological protection, medical physics, nuclear safety and criticality, analysis, and design of detectors, among others [1].

The code simulates events by accessing its various libraries consisting of photon / electron / neutron cross sections for many atoms. Physical processes that can be simulated with MCNP are coherent and incoherent scattering, fluorescence emission after photoelectric absorption and absorption in the production of pairs. Due to its versatility, MCNP allows the user to develop the model of an experiment and change the parameters to reach the ideal model desired [2].

1.2. Mass attenuation coefficient

In the nuclear engineering context, the attenuation coefficient, represented by the letter μ, is a measure of the attenuation of a particle beam's intensity passing through a slab of material. Denser materials scatter/absorb more particles, thus yielding higher attenuation coefficients. To remove the dependence on density, the coefficient is usually divided by the density value, which results in the mass attenuation coefficient $\mu_m = \mu/\rho$. The calculation of the mass attenuation coefficient can be obtained using the Beer-Lambert's equation, given in Eq. 1. To validate the mass attenuation coefficient values calculated from MCNP results, the XCOM database, available online at the National Institute of Standards and Technology (NIST) site [3], was used.

In XCOM database, it is possible to obtain photon cross section data for a single element, compound, or mixture (a combination of elements and compounds) for energies between 1 keV and 100 GeV [3], therefore it is frequently used to calculate total attenuation coefficients.

$$I = I_0\, e^{-\mu x} \tag{1}$$

where I_0 and I are respectively the incident beam and beam passing through the material, μ the total attenuation coefficient and x the thickness of the absorber material. For the equation to be used, the source must be monoenergetic and with a monodirectional beam. For this work, different geometries were evaluated in order to, later on, reproduce it in an experiment using low activity sources. The energy of the source, thickness of the sample, and the use of collimators in the source and in the detector were considered.

2. MATERIALS AND METHODS

2.1. Study of the geometry

To evaluate which geometry would be more adequate, two models were developed. In the first case, both the source and the detector were collimated with lead pieces with the same aperture diameter (4 mm) and the thickness (40 mm), with an isotropic source model. For the second case, only the detector was collimated with the lead piece, while the emission direction of source was restricted by a cone centered around the source-detector axis, creating a *virtual collimation*. A schematic of the first case is shown in Fig. 1, containing a sealed radioactive source, two lead collimators, a 1 cm-thick sample, and a 1.5"-diameter NaI(Tl) scintillation detector with aluminum enclosure.

All geometry measures were chosen to match available equipment in our laboratory. In future works, very thin plastic cups will be used as containers for liquid samples, and 3D printed PLA support for solids. In either case, the support should not interfere with the source beam. Thus, the support can be omitted from the simulations.

Figure 1: Developed geometry for first case.

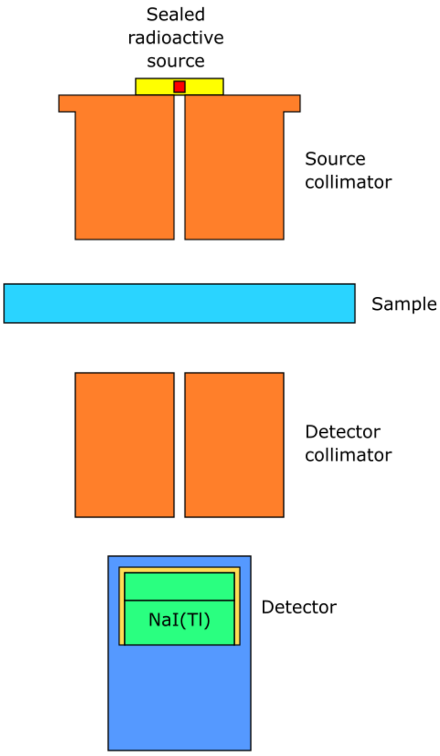

2.2. MCNP parameters

The tally chosen was F8, corresponding to the pulse height distribution (PHD) providing the energy deposition in the chosen cell (the NaI(Tl) cylinder). From the resulting PHD, the height of the peak located at the same energy as the simulated source corresponds to the attenuated beam intensity I. An additional simulation was performed without sample to obtain the incident beam intensity I_0. Those values were used calculate the mass attenuation coefficient for each type of material. Four source energies were used from the main gamma emissions of the radioactive isotopes ^{241}Am (59 keV), ^{133}Ba (81 keV and 356 keV), and ^{137}Cs (662 keV). 10^8 events (photons) were generated for each simulation. Considering each geometry, material, and source energy, a total of 32 simulations were performed sequentially on PC with a Pentium G4560 3.50 GHz processor and 12 GB RAM.

2.3. Materials and Methods

The characteristics of the chosen materials were obtained in the compendium of materials [4], whose values and composition are shown in Table 1. The materials were chosen because their densities are different at the decimal level, starting with an element: aluminum; a known compound: water; and finally, a mixture: artificial seawater, represented by the mixture of water with its largest saline component, sodium chloride. For artificial seawater, the amount of salts is 3.5%, representing the totality of salts dissolved in seawater (Salinity 35, equivalent to 35 g of salts dissolved in 1 L of seawater) [5].

Table 1: Materials investigated in this study

Material	Composition	Formula	Density (g/cm^3)
Element	Aluminum	Al	2.698900
Compound	Water	H_2O	0.998207
Mixture	Artificial seawater	H_2O + salts	1.023343

3. RESULTS AND DISCUSSION

The results obtained for the three materials (Al, H_2O, H_2O+salts) and the first geometry, using source and detector collimators are shown in Tables 2, 3 and 4. For each case, the mass attenuation coefficient was calculated. To compare the values with the reference values from XCOM, the relative error (Eq. 2) was used,

$$\text{Relative error (\%)} = 100\left|\frac{\mu_{sim} - \mu_{XCOM}}{\mu_{XCOM}}\right| \quad (2)$$

where μ_{sim} and μ_{XCOM} are the mass attenuation coefficients obtained through simulation and the XCOM database, respectively. The relative propagated error $\sigma_{\mu sim}/\mu_{sim}$ (RPE) was also calculated for each case.

Comparing with the values from XCOM, most values are close to the reference ones (RE $<$ 10%) but not precise ($\sigma_{\mu sim}/\mu_{sim} \gtrsim 10\%$). In this case, the statistics are poor due to the very low number of photons reaching the detector per emitted photon, which is in the order $\mathcal{O}(10^{-5})$. At least half the photons are generated towards the opposite direction of the detector, and the other half is mostly absorbed by the source collimator. The total simulation time was 3h 10min, showing this geometry is only adequate for a crude estimation of the mass attenuation coefficients.

Table 2: Mass attenuation coefficients for Al with isotropic source and both collimators

Source	Energy (keV)	I_0	I	μ_{sim} (cm²/g)	μ_{XCOM} (cm²/g)	Relative error	$\frac{\sigma_{\mu sim}}{\mu_{sim}}$	Time (min)
Am	59	2676	1271	0.27586	0.28080	1.8%	5%	10.1
Ba-1	81	4131	2492	0.18727	0.19960	6.2%	5%	10.2
Ba-2	356	1057	824	0.09227	0.09730	5.2%	19%	12.4
Cs	662	408	329	0.07974	0.07466	6.8%	34%	13.6

Table 3: Mass attenuation coefficients for H_2O with isotropic source and both collimators

Source	Energy (keV)	I_0	I	μ_{sim} (cm²/g)	μ_{XCOM} (cm²/g)	Relative error	$\frac{\sigma_{\mu sim}}{\mu_{sim}}$	Time (min)
Am	59	2676	2205	0.19394	0.20660	6.1%	15%	10.2
Ba-1	81	4131	3450	0.18047	0.18290	1.3%	13%	10.2
Ba-2	356	1057	941	0.11646	0.11110	4.8%	39%	12.4
Cs	662	408	368	0.10337	0.08574	20.6%	70%	13.6

Table 4: Mass attenuation coefficients for Seawater with isotropic source and both collimators

Source	Energy (keV)	I_0	I	μ_{sim} (cm²/g)	μ_{XCOM} (cm²/g)	Relative error	$\frac{\sigma_{\mu sim}}{\mu_{sim}}$	Time (min)
Am	59	2676	2197	0.19273	0.21220	9.2%	10%	10.1
Ba-1	81	4131	3469	0.17067	0.18470	7.6%	10%	10.2
Ba-2	356	1057	947	0.10738	0.11070	3.0%	12%	12.4
Cs	662	408	368	0.10083	0.08536	18.1%	14%	13.6

In the second geometry, without the actual collimator at the source, the results shown in Tables 5, 6 and 7 were closer to the XCOM values, showing it is possible to replace the source collimator for a virtual collimation of the source to obtain have values with small errors and close to the expected values.

The simulation time was approximately twice the first case, 6h 27min. However, the number of photons reaching the detector increased 3 orders of magnitude, while the relative errors decreased by half and relative propagated errors by 2 orders of magnitude.

Table 5: Mass attenuation coefficients for Al with virtual collimation of the source

Source	Energy (keV)	I_0 (10^3)	I (10^3)	μ_{sim} (cm²/g)	μ_{XCOM} (cm²/g)	Relative error	$\frac{\sigma_{\mu sim}}{\mu_{sim}}$	Time (min)
Am	59	1335.8	628.3	0.27947	0.28080	0.5%	0.1%	17.0
Ba-1	81	2028.3	1187.4	0.19840	0.19960	0.6%	0.1%	19.1
Ba-2	356	512.5	394.8	0.09668	0.09730	0.6%	0.2%	26.3
Cs	662	178.9	146.4	0.07418	0.07466	0.6%	0.4%	28.5

Table 6: Mass attenuation coefficients for H_2O with virtual collimation of the source

Source	Energy (keV)	I_0 (10^3)	I (10^3)	μ_{sim} (cm^2/g)	μ_{XCOM} (cm^2/g)	Relative error	$\frac{\sigma_{\mu sim}}{\mu_{sim}}$	Time (min)
Am	59	1335.8	1088.3	0.20534	0.20660	0.6%	0.2%	19.4
Ba-1	81	2028.3	1691.8	0.18176	0.18290	0.6%	0.1%	19.8
Ba-2	356	512.5	458.9	0.11061	0.11110	0.4%	0.4%	26.4
Cs	662	178.9	164.3	0.08535	0.08574	0.5%	0.8%	28.7

Table 7: Mass attenuation coefficients for Seawater with virtual collimation of the source

Source	Energy (keV)	I_0 (10^3)	I (10^3)	μ_{sim} (cm^2/g)	μ_{XCOM} (cm^2/g)	Relative error	$\frac{\sigma_{\mu sim}}{\mu_{sim}}$	Time (min)
Am	59	1335.8	1082.7	0.20529	0.21220	3.3%	0.2%	19.7
Ba-1	81	2028.3	1700.4	0.17230	0.18470	6.7%	0.1%	20.4
Ba-2	356	512.5	462.5	0.10026	0.11070	9.4%	0.4%	26.8
Cs	662	178.9	165.3	0.07719	0.08536	9.6%	0.9%	29.2

Although the statistical errors ($\sigma_{\mu sim}$) for seawater are low, the relative errors are still larger than for other materials. This can be explained by the fact that the values generated by XCOM for mixtures are also an estimation of the mass attenuation coefficients, and not their true value. The results are summarized in Table 8. In principle, the simulation time could still be decreased for the second model, and still have lower errors than the first model.

Given that more time spent in the simulation should turn into less errors (better estimates), one can think of a *simulation score* where the combination of these two quantities is ideally zero, as in Simulation time × Relative error. Higher energy photons (356 keV and 662 keV) interact less with the samples, resulting in poor simulation statistics. Seawater is a study case for which XCOM can only deliver an estimate for the mass attenuation coefficient. These cases caused the standard error of the average quantities shown in Table 8 to increase. With these considerations, one can only say that the RPE score is better for the second geometry.

Table 8: Results summary

Geometry	No. of Events	Average simulation time (min)	Average relative error	Average RPE	RE score	RPE score
Two collimators and isotropic source	10^8	11.9 ± 1.6	7.6 ± 6.0	28 ± 23	90 ± 42	330 ± 160
Detector collimator and virtual source collimation	10^8	24.2 ± 4.9	2.8 ± 3.6	0.32 ± 0.29	68 ± 51	7.7 ± 4.2

4. CONCLUSION

Two geometries were developed, based on a standard experiment to measure the mass attenuation coefficient, and simulated with different sources and materials. The first geometry is closer to a real measurement setup, in the sense that the source is isotropic and a piece of lead is used to collimate the source. However, this model is not efficient in simulations with the Monte Carlo method. At least half of the generated particles are lost, as their initial direction is opposite the detector. Most particles of the other half are absorbed by the detector's collimator. Therefore, very few particles interact with the sample and reach the detector.

The second geometry was designed to optimize the time spent in the simulation by reducing statistical errors. The detector's collimator was replaced by a virtual collimation, a cone that bounds the emission direction of the particles. In this case, almost all particles interact with the sample first and then reach the detector. Consequently, for the same number of events, Monte Carlo simulations for the second geometry lasted about twice the time for the first geometry. However, the mass attenuation coefficients were closer to the XCOM reference values, and the simulation errors decreased by two orders of magnitude.

Ideally, one should compare two models for given a target simulation time or a target precision. However, in this study, simulation scores were calculated for the two geometries and the second one has a better value for the RPE score, which relates to the precision of the mass attenuation coefficient estimate using the Monte Carlo method. For the second geometry, except for seawater, all coefficients are less than 1% different from those obtained with XCOM. The measurement and estimation of mass attenuation coefficients for seawater is being investigated by our group and will be the subject of future publications.

We conclude that the best geometry is when virtual collimation is used for the source, saving computational time, which is quite relevant in cases of geometries with more complex materials. This study was developed to assist in choosing the best geometry for future projects, seeking computational optimization, without losing the characteristics of an experiment.

ACKNOWLEDGMENT

The authors thank CAPES and CNPq for the financial SUPPORT, ENABLING the development of this work.

REFERENCES

[1] PELOWITZ, D. B. et al. "MCNPX user's manual version 2.5. 0." Los Alamos National Laboratory, v. 76, p. 473, (2005).

[2] MCNP, X. Monte Carlo Team, MCNP–A General Purpose Monte Carlo N-Particle Transport Code, Version 5. LA-UR-03-1987, Los Alamos National Laboratory, April 2003. BERGER, M. J. et al. "NIST standard reference database 8 (XGAM)", http://physics.nist.gov, (1990).

[3] MCCONN, R. J. et al. "Compendium of material composition data for radiation transport modeling". Pacific Northwest National Lab. (PNNL), Richland, WA (United States), 2011.

[4] MILLERO, Frank J. Chemical Oceanography. CRC Press. (Fourth edition, 2013).